

# A New, FEM-friendly Way to Predict the Endurance of Parts of Notch Sensitive Material

Kim Ravn-Jensen

Alfa Laval Copenhagen A/S,  
Søborg, Denmark

## Summary

A new method to include the influence of notch sensitivity and size effect on fatigue analysis results is presented. The method could be implemented as an automatic postprocessing procedure with a minimum of choices to be made by the user. A special, least-squares strategy makes it possible to use available fatigue test data with no need to investigate for new properties.

## Keywords

Fatigue, endurance, notch sensitivity, size effect

## 0. Introduction

The rotating parts of a decanter centrifuge must be able to withstand an unlimited number of ordinary load cycles. Therefore, a number of well-known techniques dealing with a limited fatigue life have no relevance in this context. As certain decanter components are loaded cyclically on top of a static stress state with tension and in addition have complex geometry, the relevant analytical procedures are Haigh diagramme look-up and notch sensitivity assessment.

These procedures have been well developed for simple stress states and geometries, so the challenge is to translate between the simple conditions of test specimens and the complexity of real life problems. The translation of complex stress states into uniaxial ones has been the subject of much research work ([1], [2]), and a FE-based automatization of such procedures is offered by many software vendors.

General procedures to determine how arbitrarily shaped stress concentrations affect endurance are far less available. The very term "notch sensitivity" suggests that established paradigms do not go well with today's availability of the FEM: A lab engineer will divide the applied load with the cross-sectional area and call a material "notch sensitive" if the endurance is surprisingly low. On the other hand, if the maximum stress from a FE solution is used, the endurance will generally be higher than expected. More appropriately, the distinctive material property associated with this phenomenon should be called "notch insensitivity".

Markedly notch insensitive materials tend to be "bad materials" like cast iron. As such materials may be cheap and possess other interesting properties (e.g. tribological), there should be a general need for consistent, FE-based tools in this area.

This paper describes the application of such a technique in order to predict the endurance of the large end hub of a decanter centrifuge.

## 1. A decanter centrifuge and its large end hub

Figure 1 below shows the essential parts of a decanter centrifuge:

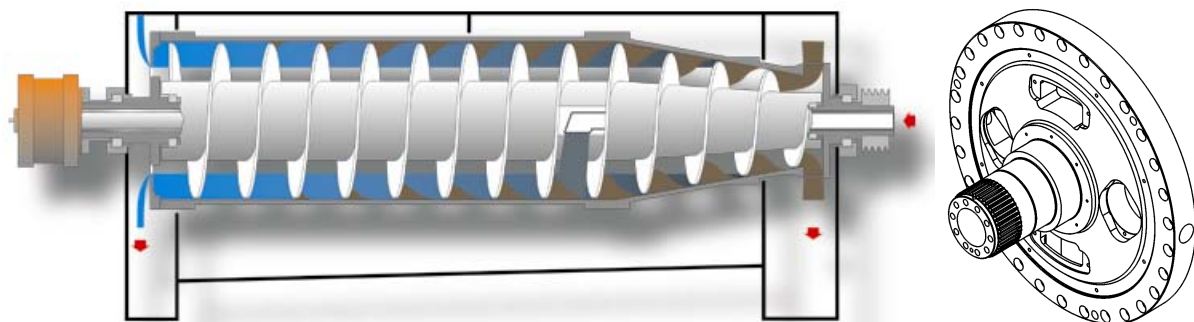


Figure 1: The basics of a decanter centrifuge (left), and a large end hub (right).

The red arrow inward to the right marks the slurry inlet (the main drive pulley is seen just left of it). The arrow down right marks the sludge outlet, and the arrow down left shows how the liquid leaves through the large end hub.

The large end hub serves a number of purposes: It supports the bowl that encapsulates the entire process, it supports the spiral shaped conveyor, and one or two liquid phases must pass through it in a controlled fashion.

## 2. Stresses in a large end hub

The high rotational velocity of the large end hub creates rather high average stresses due to liquid pressure and centrifugal forces. In addition, the influence of gravity between the main bearings,

unbalance forces and certain process effects generate variable stresses in the hub. Figure 2 and Figure 3 show contour plots for the average and the variable stress state, respectively.

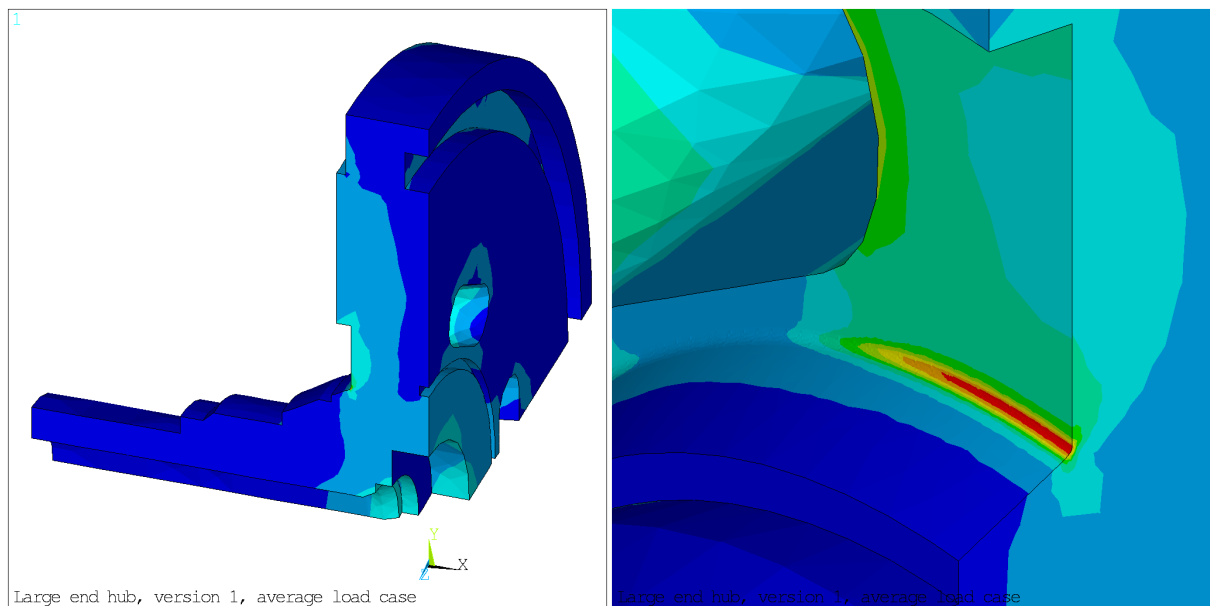


Figure 2: Von Mises stress contours illustrating the average stress state of a large end hub.

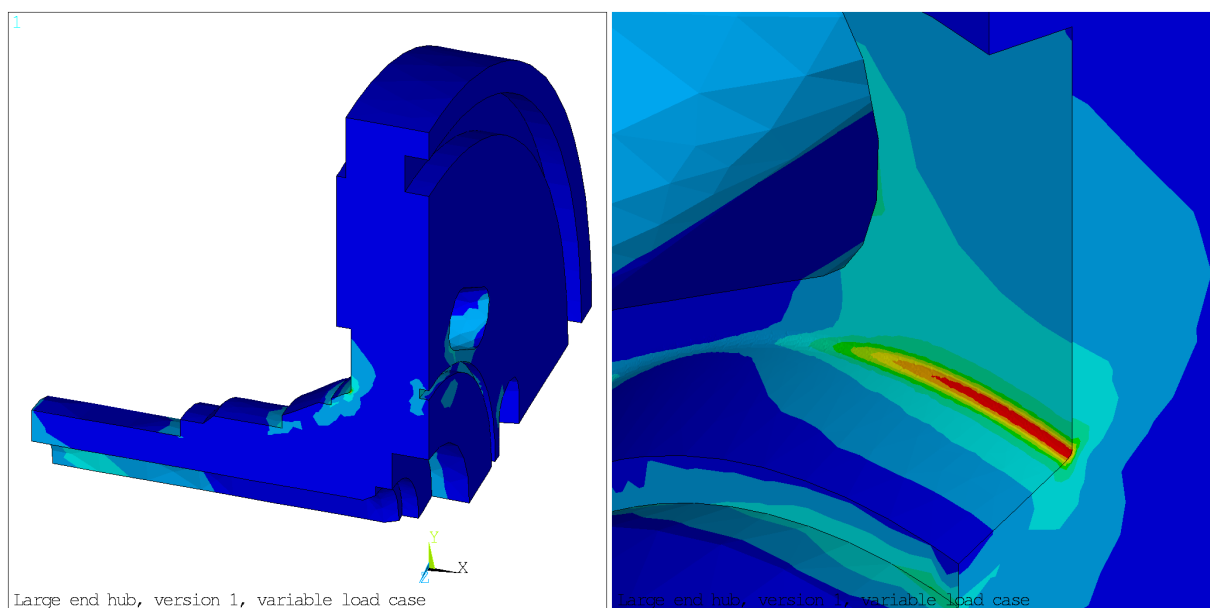


Figure 3: Von Mises stress contours illustrating the variable stress state of a large end hub.

### 3. Experimental fatigue data

To be able to consistently optimize its designs, Alfa Laval has established a database of proprietary fatigue testing results. For the endurance assessment case to be presented here, the following data were available:

Table 1: Available fatigue data.

Stress ratio $\sigma_{\min} / \sigma_{\max}$	0	0	0.5	0.65
Shape factor $K_t$	1	2.68	2.68	2.68
Average stress (MPa)	226.5	198.5	355.5	430.7
Variable stress (MPa)	226.5	198.5	118.5	91.4

#### 4. Interaction between average and variable stresses

A closer inspection of the stress states of Figure 2 and Figure 3 shows that the stress state at the critical spot shown to the right is almost uniaxial with a stress ratio of about 70 %. This should be kept in mind when selecting a suitable model for transforming the 3D stresses of the FE solution into scalar equivalents.

Ref. [1] gives you a choice between the Stress Intensity Hypothesis (SIH) and the Normal Stress Hypothesis (NSH). In brief, the SIH is based on a linearization about a stress ratio of -1 followed by integration over a half-sphere of possible normal vectors. For the NSH, all normals on a half-sphere are scanned to find the vector that gives a normal average stress and a normal variable stress closest to the limit curve of the Haigh diagramme.

To keep things simple, the limit curve is assumed to be entirely linear. Its slope is then a constant independent of any correction factors applied to the fatigue limit data. Figure 4 below shows the result of testing the SIH and the NSH hypotheses on the three rightmost columns of Table 1.

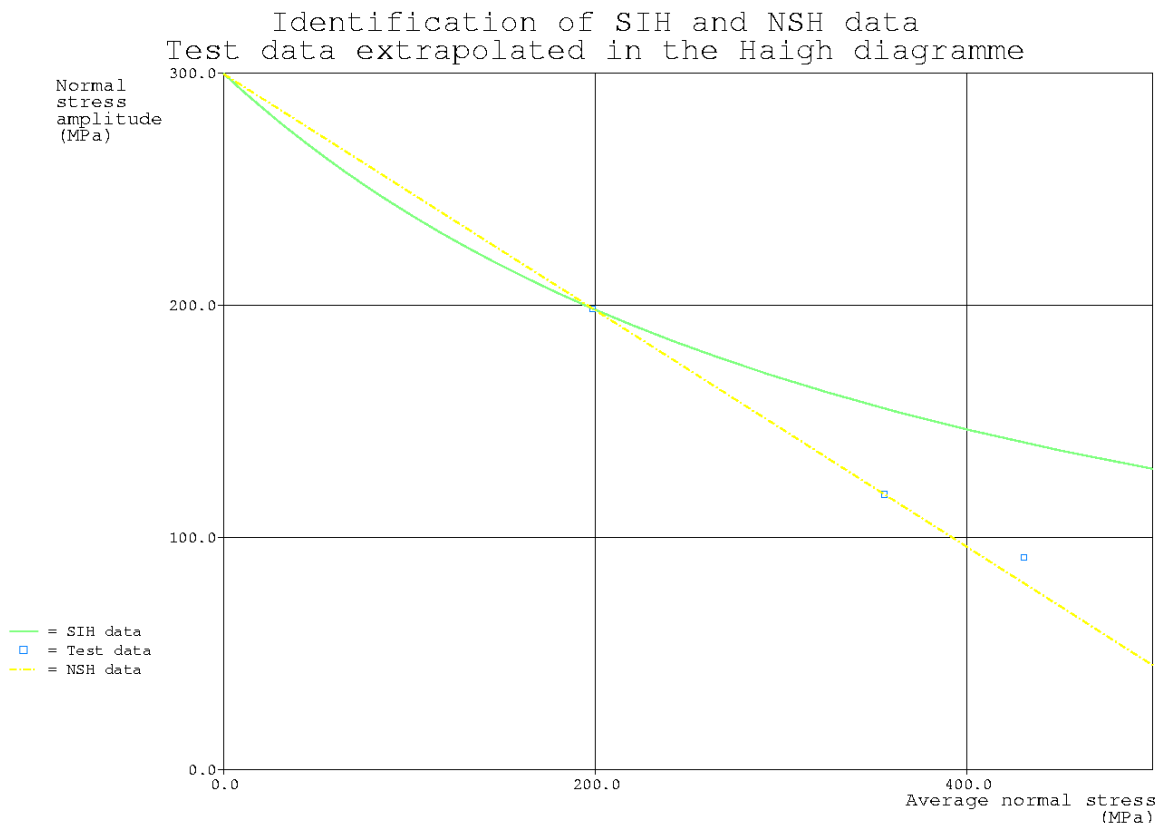


Figure 4: The SIH and NSH hypotheses are applied to the  $K_t = 2.68$  -entries of Table 1.

The SIH-procedure needs data for a stress ratio of  $-1$ . These are obtained by extrapolation of the Table 1-points for stress ratios of 0 and 0.5.

The curves of Figure 4 were calculated for a state of uniaxial tension. The SIH-curve is seen to make a non-conservative turn for stress ratios higher than 0.5. It is no wonder that the NSH-curve is a straight line: The “winning normal vector” always points in the direction of the applied stress.

Though Ref. [1] only recommends the NSH for materials like cast iron, it has nevertheless been chosen for the present study. An accompanying benefit is the possibility of plotting the stresses of all surface nodes into a Haigh diagramme as shown on Figure 5 (the limit curve has been subjected to some corrections, making it apply for an unnotched surface):

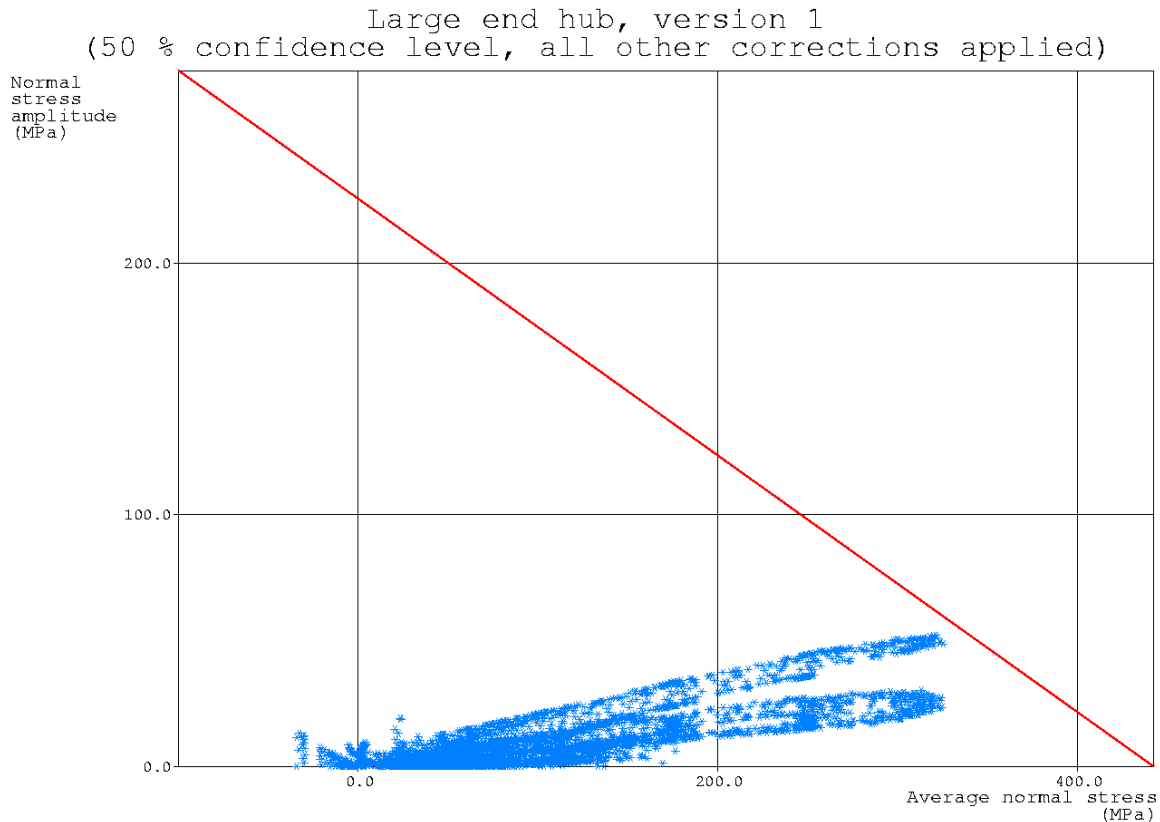


Figure 5: The stress states of Figure 2 and Figure 3 plotted into a Haigh diagramme. The two blue regions that stretch towards the limit curve originate from two neighbouring, but differently loaded spokes.

## 5. Taking notch insensitivity into account – traditional method

The apprehensibility of diagrammes like Figure 5, as offered by a number of fatigue software packages, should be seen as somewhat deceptive. Notch insensitivity should be taken into account. “Notch insensitivity” is the phenomenon that the endurance may be higher than predicted by plots like Figure 5. Using traditional methods, the highest FE-calculated stresses should be multiplied with the factor  $K_f / K_t$ . Here,  $K_f$ , the fatigue notch factor, depends on both the material and the current geometry, and  $K_t$  depends on the current geometry and the load pattern.

This is rather bewildering, and an engineer wishing to take notch insensitivity into account will frequently have doubts about which choices to make. In traditional thinking,  $K_t$  is the ratio between the high FE stress and “the stress that would have been there if the intended load had been evenly distributed”. Figure 6 shows how the path plot feature of ANSYS was used in an earlier study of the large end hub considered in this paper.

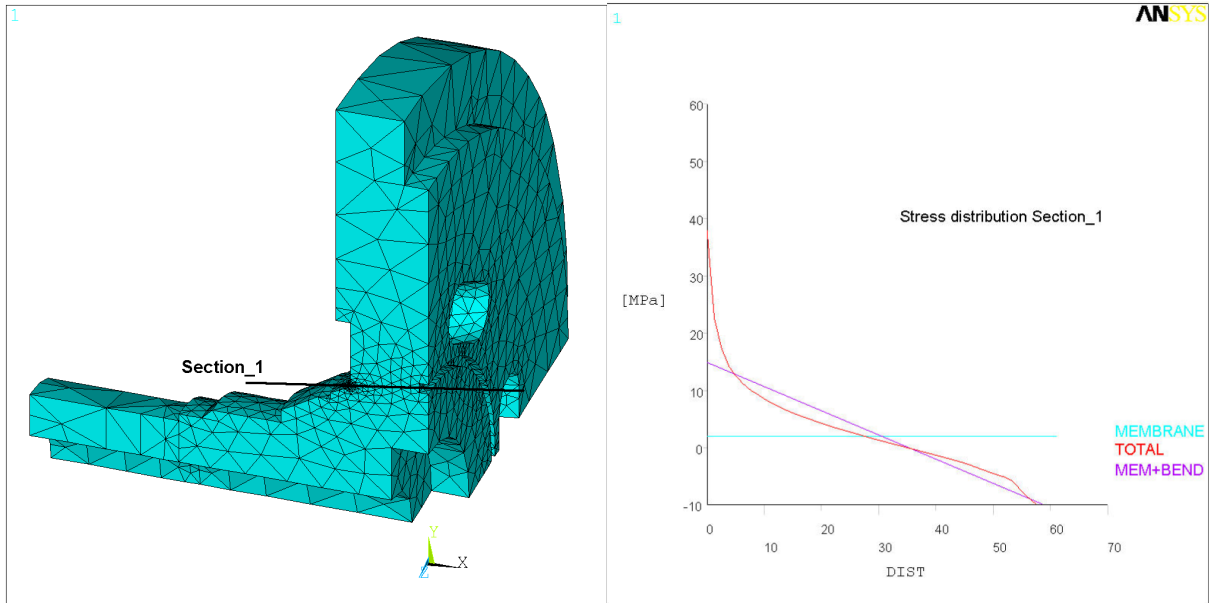


Figure 6: An attempt to evaluate  $K_t$  from a finite element solution. On the picture to the left, the stress evaluation line has been extended outside the cross section for clarity.

According to the earlier study,  $K_t$  is  $36/15=2.4$  because, from the curve plot of Figure 6, the red curve of FE stresses intersects the y-axis at  $y=36$  and the purple line intersects at  $y=15$ .

Not all corrections following the stage of Figure 5 should be expected to be conservative. If the part is bigger than the test specimens, the size effect must be accounted for. Which volume to assign to the part is then another, open question.

## 6. Taking notch insensitivity into account – new method

### 6.1 Basic theory

The “new method” to be presented here relies heavily on the work of Rabb [3], who derives his formulae by means of reliability theory.

Rabb’s procedure sets off with the notion of a “reference fatigue experiment” where a surface area  $A_{ref}$  is subjected to a cyclic stress  $\sigma_{ref}$ , at which it has a probability of fatigue failure of 0.5, or, in Rabb’s terminology, a reliability of 0.5 (one minus the probability of failure).

Another concept of Rabb’s is that the relative standard deviation of the fatigue stress  $\sigma_{ref}$  (the standard deviation divided by  $\sigma_{ref}$ ) is a material property, which in the following will be called  $s_r$ .

Now, if you have another part, you will be able to determine its fatigue reliability by means of surface integration. If an area element  $dA$  is subjected to a cyclic stress level of  $\sigma$ , you should calculate the quantity

$$(1) \quad \lambda = \frac{1}{s_r} \left( \frac{\sigma}{\sigma_{ref}} - 1 \right)$$

and then

$$(2) \quad R = \frac{1}{2} \operatorname{erfc} \left( \frac{\lambda}{\sqrt{2}} \right)$$

(*erfc*, “the complementary error function”, is available from a number of sources). The reliability of the new part is then

$$(3) \quad R_{part} = \left(\frac{1}{2}\right)^{\frac{1}{A_{ref}} \int \frac{\log(R)}{\log(\frac{1}{2})} dA}$$

If you apply this procedure to the reference experiment itself, you obtain the expected value of  $R_{part} = 0.5$ .

As  $\sigma$  in Eqtn. (1) is used the distance in a Haigh diagramme between the origo and the stress point, divided by the distance (when prolonging the stress point vector) between the origo and the intersection with the limit curve. On Figure 5, the maximum value of this so-called “proximity” is 0.958. Rabb’s procedure runs straightforwardly when you know the quantities  $\sigma_{ref}$ ,  $A_{ref}$  and  $s_r$ . According to Rabb, however, these are not easy to acquire. The difficulties lie in that

- no fatigue test specimen will exhibit a sufficiently constant stress over a well-defined reference area. There will always between the gauge area and the thread be a region of increased stress.
- a precise estimate of  $s_r$  requires many more experiment repetitions than necessary to estimate the fatigue limit itself. Just taking the scatter (and divide by the mean) tends to underestimate the true  $s_r$ .

## 6.2 Theory of fatigue material data identification

The author’s contribution to Rabb’s procedure is to model the fatigue test portfolio at hand (the data of Table 1, for instance) and then determine the best-fit  $\sigma_{ref}$ ,  $A_{ref}$  and  $s_r$ , putting less emphasis on what these quantities mean in theory.

Suppose that you have N fatigue limit experiments with different geometries, but for the same material. If you apply the procedure of Eqtns. (1)-(3) using the loads which lead to a 50% probability of failure, the sum of squares

$$(4) \quad O(\sigma_{ref}, A_{ref}, s_r) = \sum_{i=1}^N (R_{part(i)} - 0.5)^2$$

is a measure of the (lack of) quality of the current estimate of  $\sigma_{ref}$ ,  $A_{ref}$  and  $s_r$ .

The author has with considerable success applied a public domain algorithm for solving least-squares problems [4]. This algorithm calculates its own derivatives by numeric differentiation, and it is therefore very easy to use. The drawback is that it does not always converge. It does, however, have a marked ability to present a solution when the number of experiments N is equal to the number of independent variables (1, 2 or 3).

## 6.3 Example of fatigue material data identification

Using the method outlined above, a fatigue strength assessment project should start with “telling the material model what you know”. In the case considered here, Table 1 shows that there are only two comparable experiments from which to determine the effect of notch insensitivity. If you load the FE models of Figure 7 (next page),

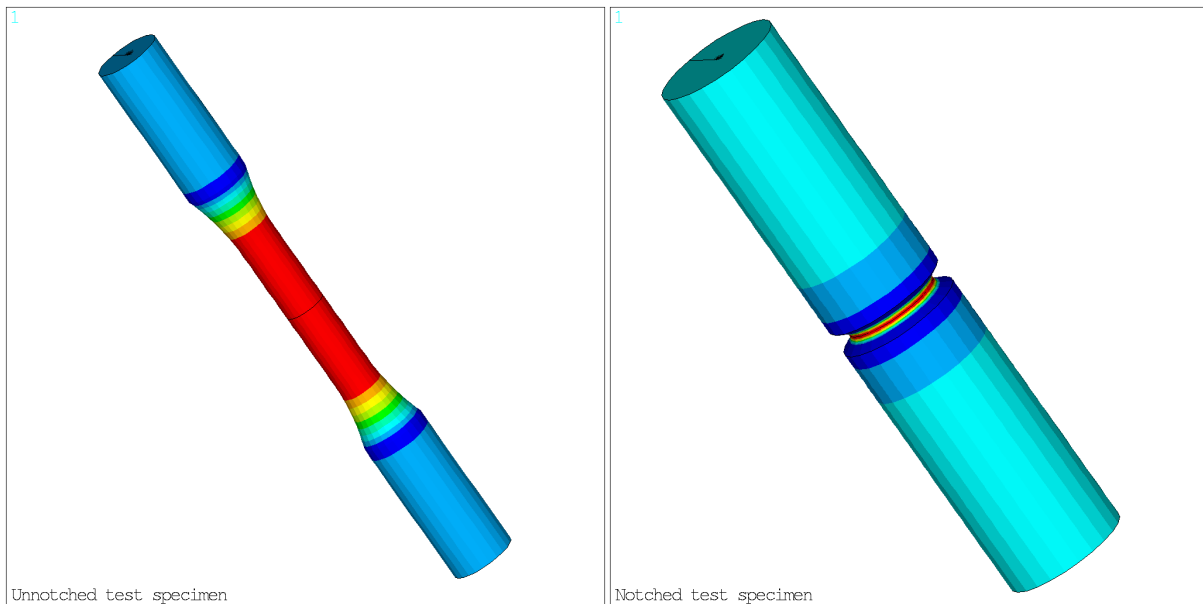


Figure 7: Axial stress contours for two of the experiments behind Table 1.

according to the two leftmost results columns of Table 1, you need one more piece of information. Following the general findings of [3],  $s_r$  was “frozen” to a value of 0.1. The least-squares algorithm then determined that a reference proximity of 0.857 and a reference area of 4585 mm<sup>2</sup> give a residual of 0 according to Eqn. (4).

#### 6.4 Results for the large end hub

Table 2 below shows the results of applying the procedure to the large end hub example. The results are given as “obtained safety factors”, i.e. factors with which to multiply the loads to reach 50% probability of failure.

Table 2: Obtained safety factors for various variations of the procedure.

	$s_r = 0.1$	$s_r = 0.05$	$s_r = 0.15$
Calibrating for each $s_r$ -value	1.150	1.154	1.143
Reusing $\sigma_{ref}$ and $A_{ref}$ from $s_r = 0.1$	1.150	1.063	1.209
Erroneously forgetting that there are 12 half-spokes	1.509	1.504	1.511
Not taking notch insensitivity into account at all	1.044	1.044	1.044

The results of the first row, “Calibrating for each  $s_r$ -value”, should be seen as a reference, against which the following rows show various ways of making things worse. It is evident that the value of the safety factor is rather insensitive to the value chosen for  $s_r$ .

The next row shows that if the values  $\sigma_{ref} = 0.857$  and  $A_{ref} = 4585$  mm<sup>2</sup> (cf. the end of Subsection 6.3) are reused for alternative choices of  $s_r$ , the stabilizing effect of matching the fatigue test data disappears, and the sensitivity to the  $s_r$ -value increases considerably.

The following row, “Erroneously forgetting that there are 12 half-spokes” emphasizes the care you have to take if you apply Eqn. (3) on, say, 1/12<sup>th</sup> of the part. This row also highlights the fact that according to the theoretical framework of ref. [3], the so-called “size effect” is the same phenomenon as notch insensitivity.

The last row of Table 2 contains three instances of the reciprocal of the maximum proximity value 0.958 referred to in Subsection 6.1 (and derived from Figure 5).

## 7. Discussion

It would not be fair to compare the upper and lower results rows of Table 2 and conclude that the new procedure really makes no difference. Firstly, the effect of a rather small hot spot area is in this particular example largely counteracted by the size effect. Secondly, the material for the large hub example considered is not as notch insensitive as, for instance, cast iron.

When the need to include notch insensitivity effects has been realized, the method presented here possesses some clear benefits:

- The basic operation is area integration, which should be numerically stable and conforms to the concepts of the finite element method.
- It is reassuring that the procedure would predict the test specimens to fail exactly the way they do.
- It is philosophically appealing that the method only considers the surface area of the analyzed part. The “traditional method” of Section 5 requires data to be extracted from the inside.
- The method is almost fully automatic. When the material data have been established, only the need to count the number of loaded instances correctly (cf. Table 2) requires some consideration from the user.

Among the drawbacks of the method is that the number of material parameters, 3, is rather one too many. Eqtn. (1) is a linearization about  $\sigma = \sigma_{ref}$  with two strange, but not prohibitive, properties:

- If the total surface area is sufficiently large (which fortunately enough is an extremely large area value), the part will break at zero stress.
- From a reference specimen, the fatigue strength of a specimen twice as big can be calculated. If from here the strength of a specimen yet twice as big is calculated, the result is different from what you would get if you from the first specimen calculate the strength of a specimen 4 times as big.

The objective of the new method is to calculate a property that is non-local and therefore cannot be displayed in a contour plot. The integrand of Eqtn. (3), may be plotted, though, to give the rightmost picture of Figure 8 below. It is seen that Eqtns. (1)-(3) “increase the contrast”.

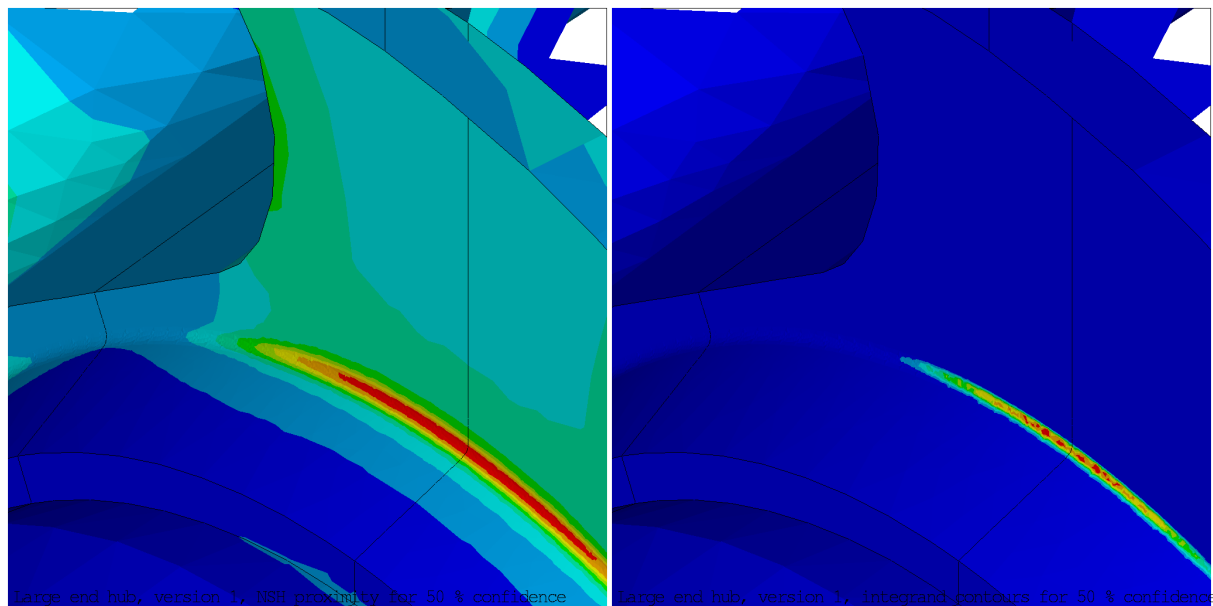


Figure 8: Contour plots of the  $\sigma$ -proximity of Eqtn. (1) (left) and the integrand of Eqtn. (3) (right).

The “obtained safety factor”-values displayed are pretty close to 1. This indicates that for this geometry and under these loading conditions, failures should be expected. Operational experience supports this prediction. Analyses of a revised design have predicted no risk of failure. Operational experience supports this prediction, too.

## References

- [1] Liu J., Zenner H.: "Berechnung der Dauerschwingfestigkeit bei mehrachsiger Beanspruchung", Mat.-wiss. U. Werkstofftech., No. 24, 1993, pp. 240-347
- [2] Zenner H., Simbürger A., Liu J: "On the fatigue limit of ductile metals under complex multiaxial loading", Int. J. of Fatigue, No. 22, 2000, pp. 137-145
- [3] Rabb B. R.: "Interpretation and evaluation of the statistical size effect", CIMAC 2001
- [4] Subroutine "Imdif.f" and dependent subroutines, developed by Argonne National Laboratory and available at <http://www.netlib.org/minpack/>